Articles

A Large Hinge Bending Domain Rotation Is Necessary for the Catalytic Function of *Escherichia coli* 5′-Nucleotidase†

Robert Schultz-Heienbrok,‡ Timm Maier,‡,§ and Norbert Sträter*,‖

Institut für Chemie/Kristallographie, Freie Universität Berlin, Takustrasse 6, 14195 Berlin, Germany, and Biotechnologisch-Biomedizinisches Zentrum der Universität Leipzig, Deutscher Platz 5, 04103 Leipzig, Germany

Received September 17, 2004; Revised Manuscript Received November 16, 2004

ABSTRACT: Two variants of *Escherichia coli* 5′-nucleotidase with disulfide bridges that were engineered to link the two domains of the protein were used to demonstrate that a large domain rotation is required for the catalytic mechanism of the enzyme. Kinetic analysis demonstrates that the variant trapped in the open form is almost inactive but can be activated up to 250-fold by reduction of the disulfide bridge. The second variant can adopt a closed but also a half-open conformation despite the presence of the cystine linkage. As a result of this flexibility, the mutant is still active in its oxidized state, although it shows a more pronounced substrate inhibition than the wild-type protein. A theoretical model is proposed that allows estimation of the flexibility of the proteins in the presence of the disulfide domain cross-link. Despite the unexpected residual flexibility of the trapped mutants, the enzymes could be used as conformational reporters in CD spectroscopy, revealing that the wild-type protein exists predominantly in an open conformation in solution. The kinetic, spectroscopic, and theoretical data are brought together to discuss the domain rotation in terms of the kinetic functioning of *E. coli* 5′-nucleotidase.

Many diverse enzymes have evolved to hydrolyze the biologically important phosphate ester linkage. These phosphatases can be classified according to their mechanism of hydrolysis as using either a nucleophilic amino acid residue or an activated water molecule as the initial acceptor of the phosphoryl group of the substrate (*1*). Many enzymes of the second category contain two adjacent metal ions in the active site (*2*). One member of this group is the periplasmic enzyme 5′-nucleotidase (5′-NT)[1] from *Escherichia coli* (E.C. 3.1.3.5 and E.C. 3.6.1.45). 5′-NT belongs to the calcineurin superfamily of dinuclear metallophosphatases, which are characterized by two sequence motifs: motif A, DXH(X)$_{\sim 25}$-GDXXD(X)$_{\sim 25}$GNH[D/E] (*3*), and a shorter motif B, GH-(X)$_{\sim 50}$GHX[H/X] (*4*).

5′-NT displays relatively broad substrate specificity. It hydrolyses all 5′-ribo- and 5′-deoxyribo-nucleotides (*5*) including bis(5′-nucleosidyl)polyphosphates (*6*) as well as uridine diphosphate sugars (*7*) and the synthetic compounds bis(*p*-nitrophenyl)phosphate and *p*-nitrophenyl phosphate (*5*). The enzyme thus cleaves both terminal phosphate ester and phosphate anhydride bonds. The biological end of the broad substrate specificity of 5′-NT might be the hydrolysis of diverse extracellular nucleotides to enable uptake of nucleosides and phosphate into the cell (*8*). The homologous ecto-5′-NT in mammalian organisms displays similar substrate specificities and is involved in a wide range of physiological processes (*8*−*10*).

5′-NT is a monomeric protein consisting of a larger N-terminal domain linked by an α-helix to a smaller C-terminal domain (*11*). The binding pocket for the substrates is located on the C-terminal domain, whereas the catalytic site with the ligands for the metal ions is located on the N-terminal domain at the C-terminal end of two sandwiched $\beta\alpha\beta\alpha\beta$ motifs that have also been described for other members of the calcineurin superfamily (*12*−*14*). Strikingly, in the first structure determined, the substrate was found to bind ∼20 Å away from the catalytic dinuclear metal center in a catalytically noncompetent manner. The assumed domain rotation could later be confirmed by an analysis of nine independent conformers from four different crystal forms (*15*). In these four crystal forms, the wild-type protein crystallized either in an open form or in a closed form with a maximum rotation of 96° and a minimum rotation of 82° between both forms. The movement can be classified as a hinge-bending domain rotation (*16*, *17*). In contrast to the classical closure motion where the domains rotate around an axis that is perpendicular to a line connecting the domain

† This work was supported by the Deutsche Forschungsgemeinschaft.

* To whom correspondence should be addressed. Tel.: 0341/9731311; fax: 0341/9731319; e-mail: strater@bbz.uni-leipzig.de.

‡ Freie Universität Berlin.

‖ Biotechnologisch-Biomedizinisches Zentrum der Universität Leipzig.

§ Present address: Institute for Molecular Biology and Biophysics, Hoenggerberg, HPK building, ETH Zuerich, CH-8093 Zuerich, Switzerland.

[1] Abbreviations: 5′-NT, 5′-nucleotidase; AMP, adenosine-5′-monophosphate; AMPCP, 5-(α,*β*-methylene)diphosphate; ATP, adenosine-5′-triphosphate; Ap4A, P1,P4-di(adenosine-5′)tetraphosphate; CD, circular dichroism; DTT, dithiothreitol; EDTA, ethylendiamin-tetraacetate; pNPP, para-nitrophenyl phosphate; 5′NT-C, double mutant Pro-90 → Cys and Leu-424 → Cys; 5′NT-O, double mutant Ser-228 → Cys and Pro-513 → Cys; wt, wild-type protein including a 6X His-tag.

10.1021/bi047989c CCC: $30.25
Published on Web 01/27/2005

centers, the C-terminal domain of 5′-NT rotates around an axis that connects the domain-linking helix and the center of the C-terminal domain. This results in a sliding motion of residues at the interface between the two domains. Nonetheless, the conventional terminology is maintained here, and we refer to the catalytically competent form as closed and to the catalytically inactive form as open.

Since 5′-NT crystallizes in the closed state both in the presence and in the absence of an inhibitor, it was assumed that the enzyme in solution exists in equilibrium between both conformations. To address this question and to assess the role of the domain rotation in catalysis, we have prepared two mutant proteins that trap the enzyme in distinct conformations by engineered disulfide bridges. The structures of both enzyme variants have been determined by X-ray crystallography (*18*). Formation of intramolecular disulfide bridges has been independently confirmed by thiol titration and gel filtration. The double mutant P90C, L424C (further on referred to as 5′NT-C) was designed to arrest the domains in a closed state. However, the X-ray structure analysis showed that the protein is indeed present in an intermediate conformation (Figure 1B), which differs by an interdomain rotation angle of 43.2° from the closed state. The double mutant S228C, P513C (referred to as 5′NT-O) did match the open conformation it was designed to (Figure 1A), although the crystallographic data indicate also some residual flexibility.

Here, we analyze the domain motion and its function for the catalytic activity of the enzyme by kinetic and spectroscopic studies of the wild-type enzyme and variants trapped in distinct conformational states. Model calculations based on the crystallographic structures of the variants further explain the observed kinetic data.

EXPERIMENTAL PROCEDURES

Cloning and Protein Production. A detailed protocol for cloning, mutagenesis, overexpression, and protein purification has been published elsewhere (*18*). To avoid contamination with chromosomally encoded wild-type protein, a 6X-His tag has been cloned C-terminally to the wild-type protein. No differences were observed between the wild-type and the His-tagged protein (which is itself herein referred to as wild-type protein). After purification, the protein was dialyzed against a 20 mM TrisHCl buffer (pH 7.4) containing 50 mM EDTA and 50 mM KCl. To determine residual metal contamination, atom absorption spectroscopy was performed (Zentrum für Proteinanalytik, Bingen). A protein/metal ion molar ratio of 0.03 for Zn^{2+} (with an error of 5%) and 0.07 for Ni^{2+} (with an error of 4%) was found. Protein concentration was determined spectrophotometrically at 280 nm using a molar absorption coefficient of 66830 M^{-1} cm^{-1} (*38*).

Enzyme Kinetics. Phosphate hydrolysis was determined by detection of inorganic phosphate (P_i) according to Van Veldhoven and Mannaerts (*39*). All reactions were carried out at 25°. The enzyme was diluted in 20 mM TrisHCl buffer (pH 7.5) containing 0.5 mM EDTA and 50 mM KCl. The reaction volume was 900 μL. The reaction was stopped with 100 μL of 4.5 M H_2SO_4. P_i was complexed for 2 min and 30 s with 200 μL of 1.75% (w/v) ammonium heptamolybdate (Riedel-Haën) in 0.9 M H_2SO_4. A total of 200 μL of 0.035% (w/v) malachite green (Sigma) in 0.35% (w/v) poly(vinyl alcohol) (M_r = 72 000, Fluka) was used for color development. After 20 min, the color was stable, and the samples were measured at 610 nm using a Shimadzu UV-160A spectrometer. Each data point represents the mean of four independent reactions. Errors are given as standard deviations. All substrates were purchased from Sigma. Steady-state kinetic parameters for the hydrolysis of AMP were determined by least-squares fitting of the initial rates using the equation $v_0 = V_{max}[S]/K_m + (1 + [S]/K_i)[S]$, where v_0 is the initial velocity, [S] is the substrate concentration, V_{max} is the maximal velocity, K_M is the Michaelis constant, and K_i is the inhibitor constant. The parameters for the hydrolysis

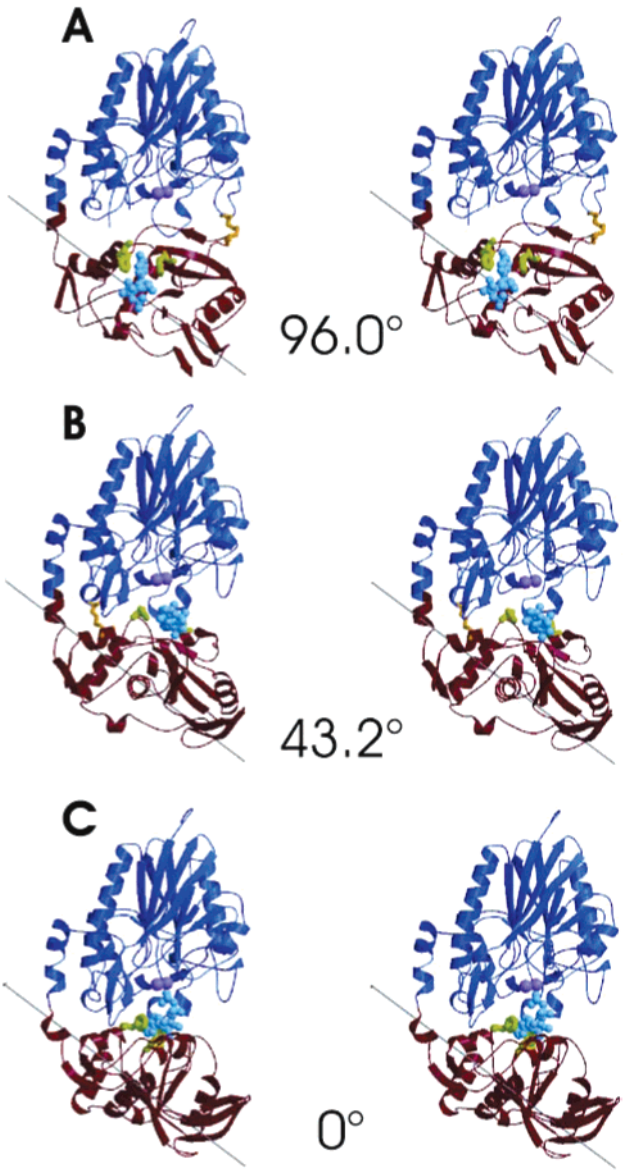

FIGURE 1: Structure of 5′-NT and its trapped mutant variants (stereoview). The N-terminal domain of the protein is drawn in blue, the C-terminal domain is in red. To follow the rotation around the axis (gray line), a substrate is drawn in light blue bound to two phenyl residues of the binding pocket (green). The engineered disulfide bridge is drawn in yellow. The position of the substrate (ATP) is modeled in analogy to the binding mode in the wild-type structure (PDB 1hp1) by a superposition based on the C-terminal domains. (A) Enzyme trapped in an open conformation (5′NT-O). (B) Enzyme trapped in an intermediate conformation (5′NT-C). (C) Most closed wild-type conformation found so far (PDB 1hpu chain C), here arbitrarily set to 0°.

of pNPP were determined by least-squares fitting of the Michaelis−Menten equation: $v_0 = V_{max}[S]/K_M + [S]$. Reaction rates are given as catalytic constants k_{cat} ($k_{cat} = v_0/[E]$ with [E] as enzyme concentration) except for the reaction with Ap4A where the production of P_i is a multistep reaction with ADP as an intermediate product. All reactions that were used for the determination of kinetic parameters were carried out in the presence of 5 mM $CoCl_2$ (Merck) as this is the most potent activator of 5′-NT (*5*). For the comparisons of oxidized versus reduced conditions, 5 mM $MnCl_2$ (Merck) was used instead since Co^{2+} is readily complexed by dithiothreitol (DTT), which was used as a reducing agent. Prior to the reactions under reducing conditions, the enzyme was incubated for 10 min with 20 mM DTT (AppliChem). The reactions were carried out in the presence of 1 mM DTT and 760 μM of the respective substrate, although other concentrations showed the same ratio of activation/inhibition. Neither prolonged incubation times nor higher DTT concentrations could further alter the reaction. DTT had no influence on the reaction with the wild-type protein.

Circular Dichroism Spectroscopy. The far-UV spectra were obtained at the synchrotron beamline 3m-NIM-1c at BESSY in Berlin. The data were taken at 20° in 0.001 cm cuvettes with a protein concentration of 115 μM in 5 mM cacodylate buffer pH 7.4. Each protein sample was measured twice in independent runs. For each run, a spectrum was acquired between 170 and 250 nm in steps of 0.5 nm with a 5 s scan for each step. For calculation of a secondary structure, data between 185 and 245 nm were used and analyzed with the SELCON 3 program for secondary structure calculation (*40*) using the DichroWeb-Server from the Birkbeck University, London (*41*). The calculations of the secondary structure contents of the crystallographic structures were done with the program DSSP (*42*) using PDB 2ush as the input structure.

The near-UV spectra were obtained with a Jasco-600 instrument purged with a nitrogen flow. The data were taken at 20° in 1.0 cm cuvettes with a protein concentration of 18.6 μM in 20 mM TrisHCl buffer pH 7.4, containing 50 mM KCl and 0.5 mM EDTA. Each protein sample was measured twice in independent runs. For each run, a spectrum was acquired between 240 and 300 nm in steps of 0.2 nm with a scan speed of 20 nm/min. Each run is composed of five accumulations. For measurements under reducing conditions, 10 mM DTT was added. The 27.5 μM adenosine 5-(α,β-methylene)diphosphate (Sigma) was used as inhibitor (*30*). Individual baseline corrections were made for measurements of buffer only, buffer with DTT, and buffer with DTT and inhibitor. Data were analyzed with the Jasco-600 software package.

Structure Analysis and Generation of Figures. The trajectory of the domain rotation was approximated using the morph-server (*43*) with an axis of rotation relating the most closed (PDB 1hpu chain C set to 0°) and most open (PDB 1hp1, which equals then 96.1 °C) conformations. The molmorph server generates by interpolation 30 theoretical structures that lie on the trajectory of the supposed domain rotation.

In Figures 1 and 6, the N-terminal domains are all superposed to the structure 1hpu chain C. The substrate ATP is taken from the structure 1hp1 and superposed to the C-terminal domains. Coordinate superpositions were calculated with the program LSQKAB (*44*). The interdomain screw axes were calculated using the program Dyndom with a pairwise comparison of the structures (*45*, *46*). A sliding window of five residues was used to generate main chain segments for which rotation vectors were calculated. The most closed wild-type protein structure (1hpu chain C) was arbitrarily chosen as origin and set to 0°. Figures 1 and 6 were generated using the programs MOLSCRIPT (*47*) and Raster3d (*48*). Both were used with the graphical user interface MOLDRAW (N. Sträter, unpublished). Figures 2−5 were plotted with the program Origin (Microcal Software).

RESULTS AND DISCUSSION

Steady-State Kinetics. The steady-state hydrolytic activity of wild-type 5′-NT and the trapped variants has been determined in the presence of cobalt, which maximally activates the metal-free enzyme. No measurable activity was found for the hydrolysis of AMP by the 5′NT-O variant, showing that the enzyme in the open state is inactive toward natural substrates, which need to bind to the substrate affinity pocket of the C-terminal domain.

The 5′NT-C mutant has about half the activity of the wild-type enzyme. This finding came as a surprise since we expected that the enzyme designed to be locked in the closed conformation is enzymatically inactive. However, the experiment and results presented in the next sections will provide an explanation for this finding in the significant residual flexibility of this mutant. In this section, we will analyze the peculiar kinetic properties of the wild-type enzyme and the 5′NT-C mutant with respect to substrate inhibition.

When using AMP as a substrate, the 5′NT-C enzyme shows a stronger substrate inhibition with an inhibition constant of 6 mM (Figure 2A and Table 1) as compared to 23 mM for the wild-type enzyme (Figure 2B and Table 1). It has been noted earlier that 5′-NT does not follow Michaelis−Menten kinetics (*5*, *6*, *19*, *20*). Figure 2A,B shows that the data can be fitted with good approximation to a model of uncompetitive substrate inhibition according to

$$v_0 = V_{max}[S]/K_m + (1 + [S]/K_i)[S] \qquad (1)$$

This inhibition model is consistent with data by Garcia et al. who have suggested that the protein possesses a second substrate binding site (*19*). Upon saturation of a higher affinity binding site, the substrate would bind to an inhibitory lower affinity binding site, resulting in uncompetitive inhibition. However, we currently can also not exclude the possibility that the substrate inhibition is related to or influenced by the domain movement of the enzyme.

The kinetic parameters k_{cat} and K_M derived here for the wild-type protein deviate slightly from those published earlier. Here, we find a K_M value for AMP of 74 μM as compared to 45 μM reported by Ruiz et al. (*6*) and 93 μM recently found by McMillen et al. (*20*). To determine K_M, both authors used data only in the range before substrate inhibition becomes apparent. This approach applied to our data results in a K_M of 52 μM (Eadie−Hofstee), which is in good agreement with the result of Ruiz et al. The k_{cat} value reported here is at a comparable substrate concentration 650 times higher than the one determined by McMillen et al. (*20*). This is most likely due to the different metal ions used.

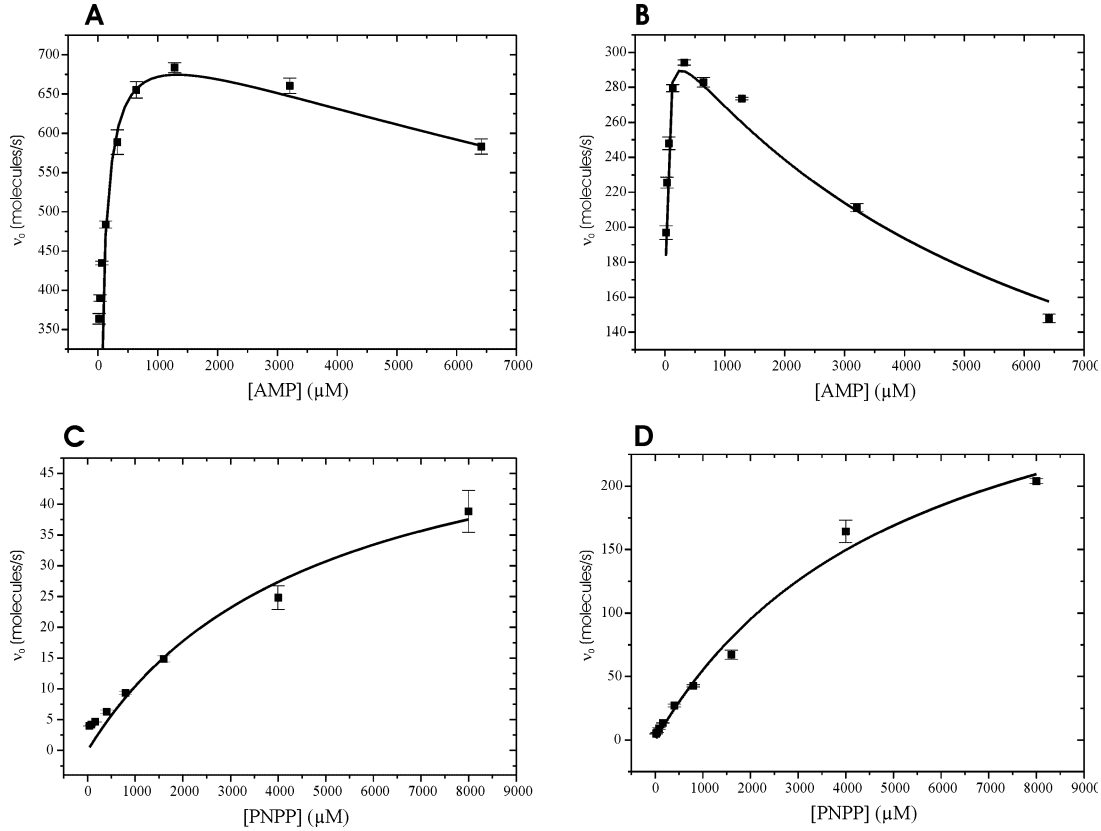

FIGURE 2: Enzymatic turnover in dependence on substrate concentration. (A) Wild-type protein with AMP as substrate. (B) 5′NT-C enzyme with AMP as substrate. (C) Wild-type protein and pNPP. (D) 5′NT-C enzyme and pNPP. The 5 mM $CoCl_2$ was added in each assay. Each data point represents a mean value of four independent measurements. The data are fitted to the Michaelis−Menten equation for the pNPP substrate and to the equation for uncompetitive inhibiton as given in the Experimental Procedures for the AMP substrate.

Table 1: Kinetic Parameters for the Wild-Type Enzyme and the 5′NT-C Variant[a]

	AMP		pNPP	
	WT	5NT-C	WT	5NT-C
k_{cat} in s^{-1}	750 ± 18	313 ± 9	60 ± 11	350 ± 40
K_M in μM	74 ± 8	11 ± 2	4741 ± 1738	5355 ± 1190
k_{cat}/K_M	10.1	28.5	0.0127	0.0654
K_I in mM	23 ± 4	6 ± 1	n.a.	n.a.

[a] All measurements were done in the presence of 5 mM $CoCl_2$.

Whereas McMillen et al. used a Zn^{2+}/Co^{2+} combination, we worked with an essentially Zn^{2+}-free enzyme (as determined by atom absorption spectroscopy) before activation with Co^{2+}. Zn^{2+} can be copurified with 5′-NT (*20*, *21*), although it has been shown to inactivate the enzyme (*5*).

The phenomenon of substrate inhibition in 5′-NT has also been observed for other natural substrates such as ADP and ATP (*19*). In contrast, the synthetic substrate pNPP shows no substrate inhibition in an equivalent concentration range (Figure 2C,D). Moreover, the K_M values of 4.7 and 5.4 mM for the binding of this substrate to the wild-type protein and the 5′NT-C mutant, respectively, are 2 orders of magnitude higher than the K_M values for AMP. This indicates that the nonnatural small substrate either binds much more weakly to the binding site or that a different, yet unidentified, binding site is used for the nitrophenyl group.

An interesting observation in the kinetics of pNPP is also that k_{cat} is higher (350 s^{-1}) in the 5′NT-C variant than in the wild-type enzyme (60 s^{-1}). This is in contrast to the hydrolysis of AMP where k_{cat} is higher in the wild-type (750 s^{-1}) than in the 5′NT-C mutant (314 s^{-1}). Apparently, the rotational constraints within the 5′NT-C enzyme only restrict hydrolysis of the natural substrate AMP but proved to be advantageous in the hydrolysis of the small substrate pNPP. Table 1 summarizes the kinetic parameters.

Flexibility of the Trapped Mutants. If the domain movement is necessary for substrate binding and product leaving, then the enzyme trapped in the closed conformation should be inactive although it resides in the catalytically competent conformation since the substrates cannot bind or products cannot leave the active site. Therefore, the high activity of the 5′NT-C enzyme came as a surprise. However, the X-ray structure determination of this variant already showed that the protein is present in an intermediate instead of a closed conformation, with an interdomain rotation angle of 43.2° half between an open and a closed form (*18*). The high activity of the 5′NT-C mutant for hydrolysis of the natural as well small synthetic substrates implies that the enzyme should also adopt a closed conformation since the AMP binding site of the C-terminal domain is more than 15 Å away from the catalytic dimetal center in the intermediate conformation, such that this cannot be a catalytically competent conformer. Furthermore, it is reasonable to assume that the 5′NT-C protein can indeed exist in a closed state since the C90−C424 disulfide bridge can adopt a low energy conformation in this enzyme form according to the SSBOND modeling calculations.

To account for this apparent flexibility in the mutant and because introducing disulfide cross-links is a common method to probe protein flexibilty (*22*−*26*), we decided to

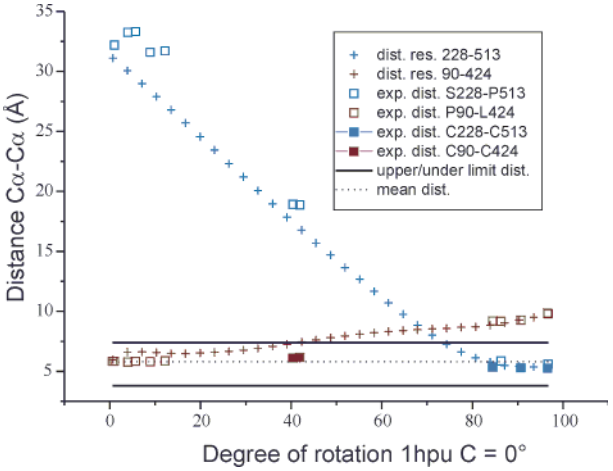

FIGURE 3: Analysis of residual flexibility in the trapped mutants. The Cα-Cα distance of the amino acid residues used to engineer the disulfide bridges is plotted against the degree of rotation. The structure 1hpu chain C is taken as reference point and set to 0°. In red are the distances of the residues 90 and 424 used to trap the enzyme in a closed conformation, in blue are the distances of the residues 228 and 513 used to trap the enzyme in an open conformation. Crosses represent the theoretical distances as inferred from a rotation of the C-terminal domain around the interdomain axis between the most open (1hp1) and most closed (1hpu C) wild-type conformations. Distances within structures of the wild-type enzyme are indicated by open squares, while that between the cysteines of the engineered variants are marked by solid squares.

further investigate the residual mobility of the trapped protein. To characterize the flexibility of this mutant with respect to a relative rotation of the two domains, we have analyzed how much the two domains might rotate around the rotation axis relating the most open and most closed conformers considering the restraints of the disulfide linkage.

A crucial parameter in disulfide bridge formation is the Cα-Cα distance of the cysteines (*27*−*29*). Figure 3 shows the calculated Cα-Cα distance between the two cysteines for a relative rotation of the two domains around the 96° rotation axis relating the most open to the most closed conformer (Figure 1). This calculation will only approximate the true motion since the trajectory of domain closure will most likely not follow a linear path (i.e., a rotation around just one axis). On the other side, the intermediate conformation analyzed in the 5′NT-C crystal structure is located approximately on this path. The analysis shows that it is likely that the C-terminal domain in 5′NT-C can move freely to a closed position (Figure 3). When the Cα-Cα distances of residues 90 and 424 of the disulfide linkage are plotted against the degree of domain rotation, it can be seen that this distance permits disulfide formation only in the range between ∼40 to 0°, which corresponds to the range between the experimental structure of 5′NT-C and the most closed structure of 5′-NT found so far. It is therefore reasonable to assume that the disulfide bridge in the 5′NT-C mutant does not restrict closing of the enzyme, whereas further opening is prohibited. In contrast, in the 5′NT-O mutant the two domains can move only within a much smaller range within the restraints of the disulfide linkage, and a complete closing of the enzyme with intact disulfide bridges is impossible. This analysis is supported by the fact that all of the experimental structures (depicted as squares in Figure 3) are in good agreement with the prediction. These calculations show that the 5′NT-C mutant is flexible between a closed and a half-open conformation. This flexibility is obviously sufficient to allow for substrate binding and product leaving.

The large rotational range of over 40° observed in the 5′NT-C protein is probably facilitated by the peculiar movement of the enzyme. In 5′-NT, the residues of the C-terminal domain slide along the domain interface rather than moving perpendiculary to it as observed in a classical hinge bending closure motion. Together with the fact that the axis of rotation runs near the disulfide bridge (cf. Figure 1B), this movement enables relatively large rotational motion by only minor geometrical distortions of the disulfide bridge.

Reduction of Engineered Disulfide Bridges. To test whether the altered kinetic pattern of the mutants is solely due to restraints in the rotational freedom of the protein or whether the mutations cause other functional distortions, we have compared the activity of the mutants under oxidizing and reducing conditions. The protein was reduced with dithiothreitol (DTT), which has no influence on the activity of the wild-type protein at the concentrations used here (data not shown). Note, however, that the less potent activator Mn^{2+} had to be used as the catalytic metal ion since Co^{2+} is strongly complexed by DTT.

Using AMP as a substrate, both enzymes can be activated with DTT (Figure 4A). The 5′NT-C variant becomes 2-fold more active and the 5′NT-O variant 250-fold. This finding indicates that both enzymes gain rotational freedom upon reduction. If the altered kinetic behavior was due to the point mutations alone, then no change upon reduction would be expected. Interestingly, the activation of the 5′NT-C enzyme is even higher for the larger substrate P^1, P^4-di(adenosine-5′) tetraphosphate (Ap4A), where the increase in activity upon reduction is 6-fold (Figure 4B). This indicates that it is more difficult for larger substrates to access the binding site of the oxidized protein, which can only adopt a half open conformation.

Reduction of the disulfide bond in the 5′NT-C enzyme actually leads to a decrease of 40% in activity toward para-nitrophenyl phosphate (pNPP) (Figure 4C). This finding indicates that the intermediate conformation already allows optimal access to the binding site for the small substrate, and hydrolysis is slowed upon reduction with DTT because the wider opening is more time-consuming or the percentage of enzyme that is present in an inactive open form increases. The 5′NT-O mutant is activated only 10-fold by the reduction when pNPP is used as a substrate. This is, however, due to the fact that the enzyme already has a relatively high turnover number in the trapped state. Most likely, for hydrolysis of the small pNPP substrate, a binding to the pocket for the adenosine moiety in the C-terminal domain is not necessary. A weak binding of pNPP to the N-terminal domain alone also explains the high K_M values observed for binding of pNPP to the wild-type and the 5′NT-C proteins (Table 1). The enhancement of the reaction rate upon reduction can be explained by the positioning of the C-terminal arginine residues (Arg 375, Arg 379, Arg 410) that most likely stabilize the transition state of the catalytic reaction (*30*). These residues cannot be moved into the active site of the 5′NT-O variant.

Usage of disulfide bridged enzymes to prove that a domain rotation is essential for the catalytic mechanism rests on the assumption that the point mutations that have been introduced to trap the enzyme do not distort the structural integrity of

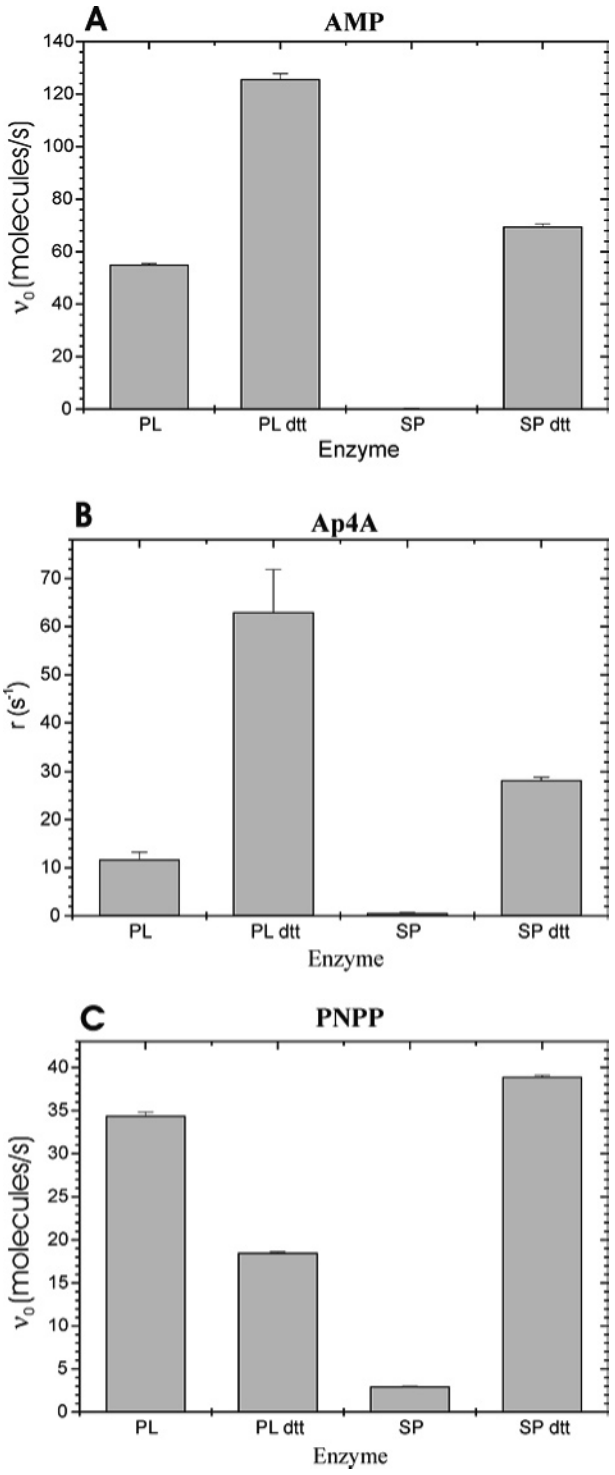

FIGURE 4: Comparison of activity of the disulfide trapped mutants under oxidizing and reducing conditions. DTT was used as reducing agent. (A) AMP as substrate. (B) Ap4A as substrate. (C) pNPP as substrate. Since hydrolysis of Ap4A occurs via at least one intermediate product, only the relative activity is obtained for this reaction in panel B by the release of phosphate. Data represent mean values of four independent measurements. All measurements were performed in the presence of 5 mM $MnCl_2$.

the protein. By determining the structures of the mutant proteins, we have shown that the introduced mutations do not cause any structural perturbances and that in particular the catalytic center remains intact. However, it is not possible to assess all influences of a point mutation structurally. Likewise, it is not possible to prove that the mutations have no other influence on the protein than to constrain its rotational freedom. Since the disulfide bridges needed to be designed at the few contact sites of the domains, it is likely that even in a reduced conformation the rotational mechanism is affected. It is therefore impossible to disentangle the effects the mutations have on the domain rotation of the protein and on other functional aspects of the protein (i.e., substrate binding and catalysis of cleavage of the ester or anhydride bonds).

CD Spectroscopy. The classical view on a domain rotation assumes that the protein exists in an open conformation until substrate binding induces closing. For many proteins, however, it could be shown that distinct conformations are present in equilibrium (*31*−*33*). An equilibrium between the closed and the open forms of 5′-NT has been assumed because the enzyme crystallizes in a closed conformation both in the absence and in the presence of an inhibitor (*30*). Studying conformational changes in solution is challenging because spectroscopic data often cannot be assigned easily to a particular conformational state. Here, the trapped conformers could serve as reference points to determine the conformation of the wild-type protein.

CD-spectroscopy is a proven tool to study conformational changes in proteins (*34*, *35*). Here, we have employed measurements of both the far and the near-UV range to test for observable conformational differences between the wild-type and the mutant proteins.

The CD spectra in the far-UV range (Figure 5A) show no significant differences. The calculated percentages of secondary structures from these data are 28.8% helix, 21.3% strand, and 22.6% turn for the wild-type protein. These data are in good agreement with the calculated secondary structure content from the X-ray structure with 29.0% helix, 20.0% strand, and 22.3% turn.

Scanning the near-UV range on the other hand reveals considerable differences in the tertiary structure between wild-type and 5′NT-O spectra on the one side and the 5′NT-C spectrum on the other side (Figure 5B). The spectra of the wild-type and the 5′NT-O protein superpose closely. The 5′NT-C spectrum is comparable to the other spectra only in the range between 285 and 275 nm and declines then steadily before it finds a plateau at 258 nm, whereas the other spectra have a trough at 266 nm and rise then again steadily up to the abrupt decline at 250 nm. The differences thus occur primarily in the region of the phenylalanines and not in the tyrosine/tryptophane range. Possibly the spectrum is strongly influenced by the C-terminal phenylalanines (Phe 429, Phe 498) that form the binding pocket for the adenosine and undergo stronger environmental changes during domain rotation.

Addition of DTT has no influence on the wild-type spectrum (data not shown) but changes the 5′NT-C and 5′NT-O spectra (Figure 5C). The slight changes in the 5′NT-O spectrum are probably due to the altered absorption of the cysteines upon reduction. Although the changes in the 5′NT-C enzyme are more pronounced, the overall shape of the 5′NT-C curve remains unchanged with a peak at 275 nm, a steady decline, and a plateau around 255 nm. We therefore conclude that the conformation of the 5′NT-C mutant in solution remains different from the wild-type enzyme even under reducing conditions. Obviously, the

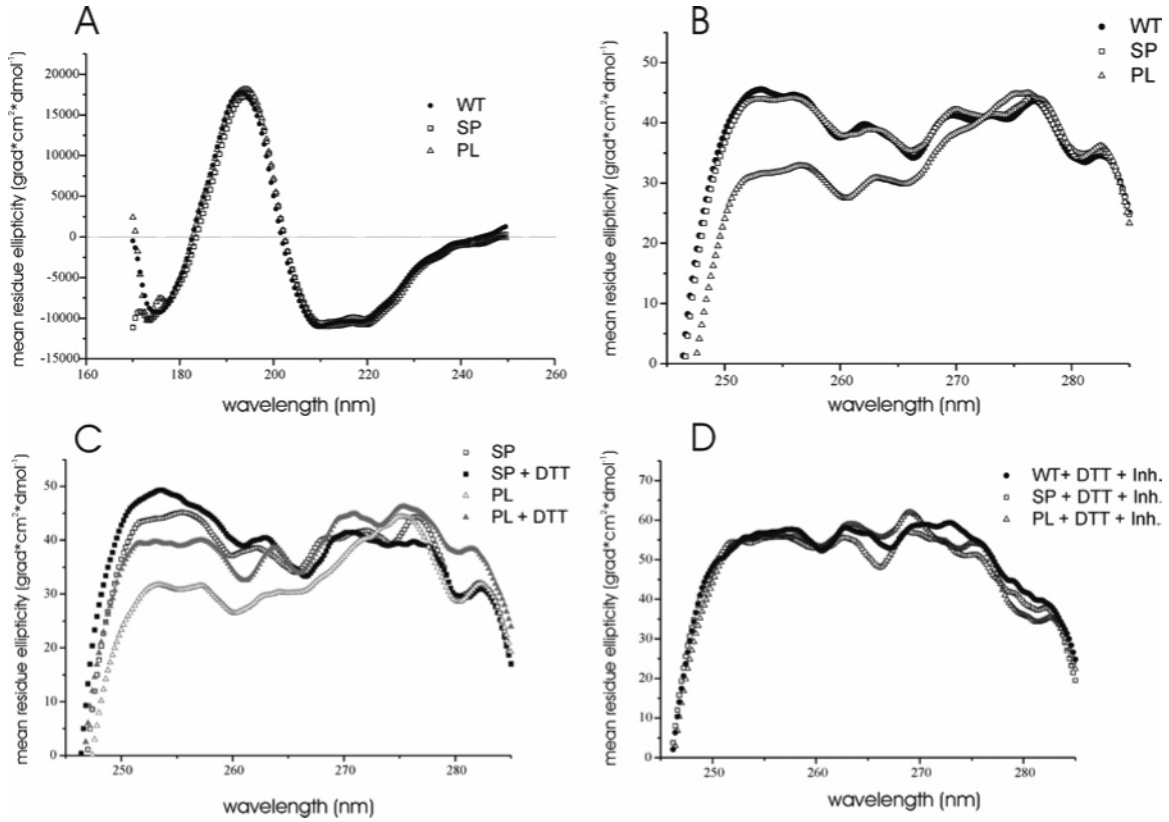

FIGURE 5: CD spectra of the wild-type protein (WT) and the disulfide bridged mutants (SP for the open conformation, 5′NT-C for the closed conformation). (A) Spectra in the far-UV range. (B) Spectra in the near-UV range. (C) The spectra of the mutant proteins with and without DTT as reducing agent. (D) Spectra with DTT and AMPCP as inhibitor. All measurements contained no metal ions in solution.

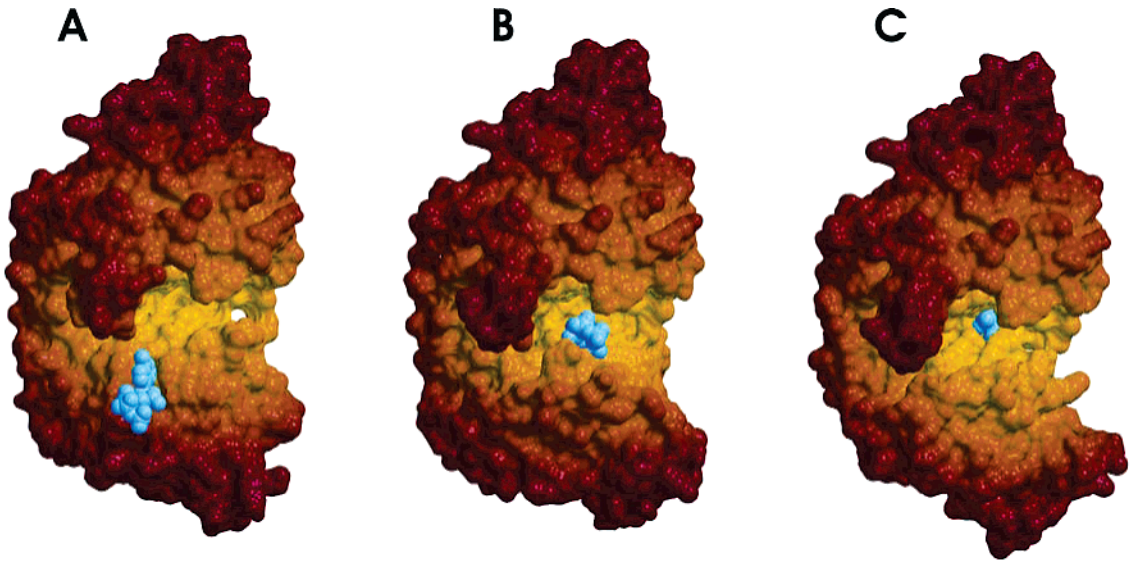

FIGURE 6: Substrate access to the binding pocket. Only the surface of the molecule and the substrate (ATP shown in blue) are drawn. The surface is colored according to the distance from the acitve site from yellow (near) to red (far away). (A) 5′-NT trapped in the open conformation (protein 5′NT-O, PDB 1oie). (B) 5′-NT in the intermediate conformation (protein 5′NT-C, PDB 1oi8 chain A). (C) 5′-NT in the most closed conformation (PDB 1hpu chain C). The position of the substrate is modeled in analogy to the binding mode in the wild-type structure (PDB 1hp1) by a superposition based on the C-terminal domains.

introduction of the cysteines at the domain interface changes the conformation of the enzyme as compared to the wild-type enzyme. Since cysteines do only weakly contribute to the spectrum, it is unlikely that the change is due to the reduced cysteines but therefore probably caused by a different orientation of the domains. Many studies confirm that reconstitution to the wild-type protein upon reduction is in most disulfide engineered proteins only partial (*23*, *24*, *36*, *37*). Evidence that the 5′NT-C enzyme nonetheless gains rotational freedom under reducing conditions is provided by the spectra obtained after addition of an inhibitor (Figure 5D). The similarity of the CD spectra of all three enzymes in the presence of DTT and the inhibitor adenosine 5-(α,*β*-methylene)diphosphate indicates that the inhibitor converts all three enzymes to a similar conformation. Since binding of the inhibitor gives itself a very strong signal that cannot

be easily subtracted by control experiments, it is difficult to assign the spectra to a particular conformation. It is likely that the proteins still assume an open conformation with the bound inhibitor because the overall shape of the wild-type and 5′NT-O spectra did not change, whereas the shape of the 5′NT-C spectrum did change.

Catalytic Cycle of 5′-NT − A Synopsis. The unexpected activity of the 5′NT-C mutant with the pronounced substrate inhibition led to interesting insights into the function of the domain rotation. Figure 6 shows a comparison of the accessibility of the substrate binding pocket in the disulfide-trapped open conformation (5′NT-O mutant, Figure 6A), the disulfide-trapped intermediate conformation (5′NT-C mutant, Figure 6B), and the most closed conformation found for the wild-type enzyme (PDB 1hpu chain C, Figure 6C). In the open conformation, the binding pocket is freely accessible from the environment, and substrates can bind and leave unhindered. In the intermediate conformation, the binding site for substrates is still accessible, but it is already buried in the inside of the protein, and substrate binding and product release is sterically hindered. In the closed conformation, substrate binding is most likely prohibited.

This is supported by the fact that activation of the 5′NT-C enzyme by DTT is higher for the larger substrate Ap4A than for the smaller AMP molecule. On top of that, the even smaller pNPP molecule can freely access the binding site in the intermediate conformation as is reflected by the high activity toward this substrate even in the absence of a reducing agent.

Further evidence in support that a full ∼96° rotation is necessary for catalysis in 5′-NT comes from comparison of the CD spectra of the wild-type protein and the 5′NT-O protein. There is ample evidence that the 5′NT-O mutant is fixed in an open conformation: (1) the protein has been shown to crystallize in the open conformation to which it was designed. Two other experimental structures assume conformations that are within a rotation of 12° from the most open conformation of 5′-NT (PDB 1hp1) (*18*). (2) Theoretical calculations on basis of the structure show that the 5′NT-O mutant cannot close by more than 15° in the presence of the cystine bridge (Figure 3). (3) The 5′NT-O mutant is inactive in its oxidized form and can be activated upon reduction (Figure 2), indicating that the trapped protein cannot spontaneously change its conformation to a closed (i.e., catalytically competent) conformation. We therefore conclude that the 5′NT-O mutant can be used as a spectroscopic reference for the open conformation. CD-spectroscopy (Figure 5) shows that the spectra of the wild-type protein and the 5′NT-O protein are identical. Because it is not possible to predict the degree of conformational difference that would result in an altered CD spectrum, the wild-type and the 5′NT-O protein might, despite their identical spectra, still assume different conformations in solution. However, by comparison with the 5′NT-C mutant that can open up only to about 50° (Figure 3), it is safe to conclude that the wild-type protein in solution assumes a three-dimensional conformation very similar to the open conformation.

If the protein needs to be in an open conformation to release the product, a mechanism of substrate inhibition becomes apparent. A second low affinity binding site might be present on the C-terminal domain for the binding of larger substrates such as diadenosine compounds. Under high substrate concentrations this second binding site is occupied and might interfere with the catalytic steps, for example, by binding to the metal ions and/or by stabilizing the closed conformation and thus inhibiting the domain movement. This second binding site has been proposed earlier on data based on different kinetics for AMP as opposed to ADP and ATP and a substrate competition plot (*19*). However, this putative second binding site still remains to be experimentally shown.

ACKNOWLEDGMENT

We thank W. Saenger for generous support as well as Peter Baumgärtel and Jan Lengefeld for their kind assistance and excellent support with measurements at the BESSY II Synchrotron.

REFERENCES

1. Vincent, J. B., Crowder, M. W., and Averill, B. A. (1992) Hydrolysis of phosphate monoesters: a biological problem with multiple chemical solutions, *Trends Biochem. Sci. 17*, 105−10.
2. Strater, N., Lipscomb, W., Klabunde, T., and Krebs, B. (1996) Two-metal ion catalysis in enzymatic acyl- and phosphoryl-transfer reactions, *Angew. Chem. Intl. Ed. England 35*, 2024−55.
3. Zhuo, S., Clemens, J. C., Stone, R. L., and Dixon, J. E. (1994) Mutational analysis of a Ser/Thr phosphatase. Identification of residues important in phosphoesterase substrate binding and catalysis, *J. Biol. Chem. 269*, 26234−8.
4. Klabunde, T., Strater, N., Frohlich, R., Witzel, H., and Krebs, B. (1996) Mechanism of Fe(III) −Zn(II) purple acid phosphatase based on crystal structures, *J. Mol. Biol. 259*, 737−48.
5. Neu, H. C. (1967) The 5′-nucleotidase of *Escherichia coli*. I. Purification and properties, *J. Biol. Chem. 242*, 3896−904.
6. Ruiz, A., Hurtado, C., Meireles Ribeiro, J., Sillero, A., and Gunther Sillero, M. A. (1989) Hydrolysis of bis(5′-nucleosidyl) polyphosphates by *Escherichia coli* 5′-nucleotidase, *J. Bacteriol. 171*, 6703−9.
7. Glaser, L., Melo, A., and Paul, R. (1967) Uridine diphosphate sugar hydrolase. Purification of enzyme and protein inhibitor, *J. Biol. Chem. 242*, 1944−54.
8. Zimmermann, H. (1992) 5′-Nucleotidase: molecular structure and functional aspects, *Biochem. J. 285* (Pt 2), 345−65.
9. Zimmermann, H. (2001) Ectonucleotidases: Some recent developments and a note on nomenclature, *Drug Dev. Res. 52*, 44−56.
10. Fini, C., Talamo, F., Cherri, S., Coli, M., Floridi, A., Ferrara, L., and Scaloni, A. (2003) Biochemical and mass spectrometric characterization of soluble ecto-5′-nucleotidase from bull seminal plasma, *Biochem. J. 372*, 443−51.
11. Knofel, T., and Strater, N. (1999) X-ray structure of the *Escherichia coli* periplasmic 5′-nucleotidase containing a dimetal catalytic site, *Nat. Struct. Biol. 6*, 448−53.
12. Strater, N., Klabunde, T., Tucker, P., Witzel, H., and Krebs, B. (1995) Crystal structure of a purple acid phosphatase containing a dinuclear Fe(III) −Zn(II) active site, *Science 268*, 1489−92.
13. Goldberg, J., Huang, H. B., Kwon, Y. G., Greengard, P., Nairn, A. C., and Kuriyan, J. (1995) Three-dimensional structure of the catalytic subunit of protein serine/threonine phosphatase-1, *Nature 376*, 745−53.
14. Kissinger, C. R., Parge, H. E., Knighton, D. R., Lewis, C. T., Pelletier, L. A., Tempczyk, A., Kalish, V. J., Tucker, K. D., Showalter, R. E., Moomaw, E. W. et al. (1995) Crystal structures of human calcineurin and the human FKBP12−FK506−calcineurin complex, *Nature 378*, 641−4.
15. Knofel, T., and Strater, N. (2001) *E. coli* 5′-nucleotidase undergoes a hinge-bending domain rotation resembling a ball-and-socket motion, *J. Mol. Biol. 309*, 255−66.
16. Hayward, S. (1999) Structural principles governing domain motions in proteins, *Proteins 36*, 425−35.
17. Gerstein, M., Lesk, A. M., and Chothia, C. (1994) Structural mechanisms for domain movements in proteins, *Biochemistry 33*, 6739−49.
18. Schultz-Heienbrok, R., Maier, T., and Strater, N. (2004) Trapping a 96° domain rotation in two distinct conformations by engineered disulfide bridges, *Protein Sci. 13*, 1811−22.

19. Garcia, L., Chayet, L., Kettlun, A. M., Collados, L., Chiong, M., Traverso-Cori, A., Mancilla, M., and Valenzuela, M. A. (1997) Kinetic characteristics of nucleoside mono-, di-, and triphosphatase activities of the periplasmic 5′-nucleotidase of *Escherichia coli*, *Comp. Biochem. Physiol., B 117*, 135−42.
20. McMillen, L., Beacham, I. R., and Burns, D. M. (2003) Cobalt activation of *Escherichia coli* 5′-nucleotidase is due to zinc ion displacement at only one of two metal-ion-binding sites, *Biochem. J. 372*, 625−630.
21. Dvorak, H. F., and Heppel, L. A. (1968) Metallo-enzymes released from *Escherichia coli* by osmotic shock. II. Evidence that 5′-nucleotidase and cyclic phosphodiesterase are zinc metallo-enzymes, *J. Biol. Chem. 243*, 2647−53.
22. Gozu, M., Lee, Y. H., Ohhashi, Y., Hoshino, M., Naiki, H., and Goto, Y. (2003) Conformational dynamics of β(2)-microglobulin analyzed by reduction and reoxidation of the disulfide bond, *J. Biochem. (Tokyo) 133*, 731−6.
23. Chervitz, S. A., and Falke, J. J. (1995) Lock on Off Disulfides Identify the Transmembrane Signaling Helix of the Aspartate Receptor, *J. Biol. Chem. 270*, 24043−53.
24. Rothery, E. L., Mowat, C. G., Miles, C. S., Mott, S., Walkinshaw, M. D., Reid, G. A., and Chapman, S. K. (2004) Probing domain mobility in a flavocytochrome, *Biochemistry 43*, 4983−9.
25. Careaga, C. L., and Falke, J. J. (1992) Thermal motions of surface α-helices in the d-galactose chemosensory receptor. Detection by disulfide trapping, *J. Mol. Biol. 226*, 1219−35.
26. Careaga, C. L., Sutherland, J., Sabeti, J., and Falke, J. J. (1995) Large amplitude twisting motions of an interdomain hinge: a disulfide trapping study of the galactose−glucose binding protein, *Biochemistry 34*, 3048−55.
27. Srinivasan, N., Sowdhamini, R., Ramakrishnan, C., and Balaram, P. (1990) Conformations of Disulfide Bridges in Proteins, *Intl. J. Peptide Protein Res. 36*, 147−155.
28. Petersen, M. T. N., Jonson, P. H., and Petersen, S. B. (1999) Amino acid neighbors and detailed conformational analysis of cysteines in proteins, *Protein Eng. 12*, 535−548.
29. Thornton, J. M. (1981) Disulphide bridges in globular proteins, *J. Mol. Biol. 151*, 261−87.
30. Knofel, T., and Strater, N. (2001) Mechanism of hydrolysis of phosphate esters by the dimetal center of 5′-nucleotidase based on crystal structures, *J. Mol. Biol. 309*, 239−54.
31. Liao, D. I., Karpusas, M., and Remington, S. J. (1991) Crystal Structure of an Open Conformation of Citrate Synthase from Chicken Heart at 2.8 Å Resolution, *Biochemistry 30*, 6031−6036.
32. Goto, N. K., Skrynnikov, N. R., Dahlquist, F. W., and Kay, L. E. (2001) What is the average conformation of bacteriophage T4 lysozyme in solution? A domain orientation study using dipolar couplings measured by solution NMR, *J. Mol. Biol. 308*, 745−764.
33. Bond, R. A., Leff, P., Johnson, T. D., Milano, C. A., Rockman, H. A., McMinn, T. R., Apparsundaram, S., Hyek, M. F., Kenakin, T. P., Allen, L. F. et al. (1995) Physiological effects of inverse agonists in transgenic mice with myocardial overexpression of the β2-adrenoceptor, *Nature 374*, 272−6.
34. Adler, A. J., Greenfield, N. J., and Fasman, G. D. (1973) Circular dichroism and optical rotatory dispersion of proteins and polypeptides, *Methods Enzymol. 27*, 675−735.
35. Greenfield, N. J. (1996) Methods to estimate the conformation of proteins and polypeptides from circular dichroism data, *Anal. Biochem. 235*, 1−10.
36. Matsumura, M., and Matthews, B. W. (1989) Control of Enzyme-Activity by an Engineered Disulfide Bond, *Science 243*, 792−794.
37. Tiebel, B., Aung-Hilbrich, L. M., Schnappinger, D., and Hillen, W. (1998) Conformational changes necessary for gene regulation by Tet repressor assayed by reversible disulfide bond formation, *EMBO J. 17*, 5112−9.
38. Gill, S. C., and von Hippel, P. H. (1989) Calculation of protein extinction coefficients from amino acid sequence data, *Anal. Biochem. 182*, 319−26.
39. Van Veldhoven, P. P., and Mannaerts, G. P. (1987) Inorganic and organic phosphate measurements in the nanomolar range, *Anal. Biochem. 161*, 45−8.
40. Sreerama, N., Venyaminov, S. Y., and Woody, R. W. (1999) Estimation of the number of α-helical and β-strand segments in proteins using circular dichroism spectroscopy, *Protein Sci. 8*, 370−80.
41. Lobley, A., Whitmore, L., and Wallace, B. A. (2002) DICHROWEB: an interactive website for the analysis of protein secondary structure from circular dichroism spectra, *Bioinformatics 18*, 211−2.
42. Kabsch, W., and Sander, C. (1983) Dictionary of protein secondary structure: pattern recognition of hydrogen-bonded and geometrical features, *Biopolymers 22*, 2577−637.
43. Echols, N., Milburn, D., and Gerstein, M. (2003) MolMovDB: analysis and visualization of conformational change and structural flexibility, *Nucleic Acids Res. 31*, 478−82.
44. Kabsch, W., Kabsch, H., and Eisenberg, D. (1976) Packing in a new crystalline form of glutamine synthetase from *Escherichia coli*, *J. Mol. Biol. 100*, 283−91.
45. de Groot, B. L., Hayward, S., van Aalten, D. M. F., Amadei, A., and Berendsen, H. J. C. (1998) Domain motions in bacteriophage T4 lysozyme: A comparison between molecular dynamics and crystallographic data, *Proteins 31*, 116−27.
46. Hayward, S., and Berendsen, H. J. (1998) Systematic analysis of domain motions in proteins from conformational change: new results on citrate synthase and T4 lysozyme, *Proteins 30*, 144−54.
47. Kraulis, P. J. (1991) Molscript−a Program to Produce Both Detailed and Schematic Plots of Protein Structures, *J. Appl. Crystallogr. 24*, 946−950.
48. Merritt, E. A., and Murphy, M. E. P. (1994) Raster3d Version-2.0−a Program for Photorealistic Molecular Graphics, *Acta Crystallogr., Sect. D 50*, 869−873.

BI047989C